Acta Crystallographica Section D
Biological Crystallography
ISSN 0907-4449

Structure of the biotin carboxylase subunit of pyruvate carboxylase from *Aquifex aeolicus* at 2.2 Å resolution

Shin Kondo,[a] Yoshitaka Nakajima,[a] Shigetoshi Sugio,[a]* Jin Yong-Biao,[b] Shinji Sueda[b] and Hiroki Kondo[b]

[a]MCC Group Science and Technology Research Center, Mitsubishi Chemical Corporation, 1000 Kamoshida-cho, Aoba-ku, Yokohama 227-8502, Japan, and [b]Department of Biochemical Engineering and Science, Kyushu Institute of Technology, 680-4 Kawazu, Iizuka, Fukuoka 820-8502, Japan

Correspondence e-mail: ssugio@rc.m-kagaku.co.jp

Received 26 September 2003
Accepted 7 January 2004

PDB Reference: BC subunit of pyruvate carboxylase, 1ulz, r1ulzsf.

Pyruvate carboxylase (PC) is distributed in many eukaryotes as well as in some prokaryotes. PC catalyzes the ATP-dependent carboxylation of pyruvate to form oxalacetate. PC has three functional domains, one of which is a biotin carboxylase (BC) domain. The BC subunit of PC from *Aquifex aeolicus* (PC-β) was crystallized in an orthorhombic form with space group $P2_12_12$, unit-cell parameters a = 92.4, b = 122.1, c = 59.0 Å and one molecule in the asymmetric unit. Diffraction data were collected at 100 K on BL24XU at SPring-8. The crystal structure was determined by the molecular-replacement method and refined against 20.0–2.2 Å resolution data, giving an R factor of 0.199 and a free R factor of 0.236. The crystal structure revealed that PC-β forms a dimeric quaternary structure consisting of two molecules related by crystallographic twofold symmetry. The overall structure of PC-β is similar to other biotin-dependent carboxylases, such as acetyl-CoA carboxylase (ACC). Although some parts of domain B were disordered in ACC, the corresponding parts of PC-β were clearly determined in the crystal structure. From comparison between the active-site structure of ACC with ATP bound and a virtual model of PC-β with ATP bound, it was shown that the backbone torsion angles of Glu203 in PC-β change and some of water molecules in the active site of PC-β are excluded upon ATP binding.

1. Introduction

Pyruvate carboxylase (PC; EC 6.4.1.1) is involved in gluconeogenesis by mediating the carboxylation of pyruvate to oxaloacetate (Jitrapakdee & Wallace, 1999; Scrutton, 1978). PC is distributed in many eukaryotes as well as in some prokaryotes. PC has three functional domains: biotin carboxylase (BC), carboxyl transferase (CT) and biotin carboxyl-carrier protein (BCCP). These domains either reside on a single polypeptide chain or constitute two subunits. The former type of PC is distributed in eukaryotes and some prokaryotes and the latter is found only in prokaryotes.

The reaction of PC and other biotin-dependent carboxylases such as acetyl-CoA carboxylase (ACC) and propionyl-CoA carboxylase proceeds in two steps. Enzyme-bound biotin is first carboxylated by bicarbonate and ATP and the carboxyl group temporarily bound on biotin is subsequently transferred to an acceptor substrate such as pyruvate or acetyl-CoA (Wood & Barden, 1977; Attwood, 1995). The first partial reaction is mediated by the BC domain or subunit and is common to all biotin-dependent carboxylases, whereas the second partial reaction mediated by the CT domain or subunit differs from enzyme to enzyme depending on the substrate to be carboxylated (Wood & Barden, 1977).

One characteristic feature of single polypeptide chain-type PCs is that their reaction is subject to allosteric regulation by acetyl-CoA and aspartate, which activate and deactivate the enzyme, respectively (Jitrapakdee & Wallace, 1999; Cazzulo & Stoppani, 1968; Attwood, 1993), whereas subunit-type PCs from bacteria do not require acetyl-CoA for activation (Cohen *et al.*, 1979; Mukhopadhyay *et al.*, 1998). This class of PC (for example that from *Aquifex aeolicus*) is made up of two subunits of molecular weight 70 and 50 kDa, while the major class (for example PC from *Bacillus thermodenitrificans*; previously known as *B. stearothermophilus*) is composed of a single polypeptide chain of molecular weight 130 kDa (Kondo *et al.*, 1997) and requires acetyl-CoA for activation (Jitrapakdee & Wallace, 1999; Barden *et al.*, 1975). The three-dimensional structure of the BC subunit of *Escherichia coli* ACC has previously been reported both alone and complexed with ATP (Waldrop *et al.*, 1994; Thoden *et al.*, 2000). In addition, the three-dimensional structure of the CT domain of yeast ACC has also been reported recently (Zhang *et al.*, 2003). Although the reaction of all BC subunits is identical and their amino-acid sequences are approximately 50% homologous among all known biotin-dependent carboxylases, the conservation of the three-dimensional structure of the BC subunit among the carboxylases is an open question in light of the difference in the susceptibility to allosteric regulation described above.

Here, we describe the three-dimensional structure of the BC subunit of PC (PC-β) from *A. aeolicus* refined to 2.2 Å resolution. Although the overall structure of PC-β is similar to the BC subunit of ACC from *E. coli* in which ATP is bound, the crystal structure clearly shows that domain B of PC-β contains no ATP in its ATP-binding pocket. We discuss three subjects in this article: the overall structure, the structure of the ATP-binding site and the comparison of the residue arrangement at the active site of ACC and PC-β.

2. Materials and methods

2.1. Construction of an overexpression plasmid for PC

An overexpression plasmid for the α (CT + BCCP; MW 70 kDa) and β (BC; MW 50 kDa) subunits of *A. aeolicus* PC was prepared as follows. The size of the α gene is 2.0 kbp and that of BC is 1.4 kbp (Deckert *et al.*, 1998). Both genes were PCR-amplified with chromosomal DNA as template. The α gene was amplified as two fragments of 800 bp and 1.2 kbp using the following primers furnished with an appropriate restriction-enzyme site: α1, 5′-CTCG**CCATGG**TCAATAGAATTCTCGTGAACAGA-3′; α2, 5′-GGC**GAATTC**TGTGC-3′; α3, 5′-GCA**GAATTC**GCCAAAATGTGC-3′; α4, 5′-CCTT**GGTACC**TTTTATAAACCGTGGTAAGCGGCTATAGA-3′ (restriction-enzyme sites are in bold). The β gene was also amplified as two fragments of 270 bp and 1.2 kbp using the following primers: β1, 5′-AAA**GGTACC**AAGGAGGTAATATAGATGGTAAACCCG-3′; β2, 5′-GTGAGA**GGATCC**GAACGCTAAGGGTGAAAGTACTGT3′; β3, 5′-TTC**GGATCC**TCTCACCCTGCAACCGAGACC-3′; β4, 5′-AAG**GTCGAC**TTATTGATAGCTCTTATCTTCTTTGTGGGG-3′. The PCR conditions described below were the same in all samples. The reaction mixture contained 5 U *Ex Taq* (Takara BIO Inc., Kyoto), 1× *Ex Taq* buffer, 200 µ*M* of each the four dNTPs, 100 pmol of each the primers and 10 ng *A. aeolicus* chromosomal DNA. After denaturation at 370 K for 5 min, the samples were subjected to 20 cycles of denaturation (370 K, 1 min), annealing (330 K, 3 min) and extension (345 K, 5 min) and subsequently subjected to additional extension (345 K, 10 min). After completion of this first PCR reaction, 5 U of *Ex Taq* was added to the samples and the above PCR cycle was repeated. The PCR products were TA cloned and sequenced. The inserts were cut out of the vector and recloned into the pTrc99A vector sequentially. The resulting plasmid carried the β and α genes in tandem and enabled simultaneous expression of the two subunits in nearly equal quantities. The co-expressed α and β subunits form a tight complex and this structure is retained throughout purification.

2.2. Expression and purification of overexpressed PC

E. coli JM109 transformed with the overexpression plasmid prepared above was grown in LB medium containing 50 µg ml^{-1} ampicillin and 1 µg ml^{-1} biotin. The harvested cells were suspended in 0.12 *M* potassium phosphate buffer pH 7.0 containing 1 m*M* EDTA, 1 m*M* DTT and 1 m*M* PMS, disrupted by sonication and then centrifuged. The supernatant cell lysate was warmed at 343 K for 30 min. The precipitate formed was removed by centrifugation and ammonium sulfate was added to the supernatant to 50–60% saturation. The precipitate formed was collected by centrifugation and dissolved in buffer *A* (10 m*M* potassium phosphate buffer pH 7.0 containing 0.1 m*M* EDTA and 0.1 m*M* DTT). The sample was subjected to gel-filtration chromatography on Superdex 200 (Amersham Biosciences). The desired fractions were collected and subjected to anion-exchange chromatography on DEAE-cellulose (Whatman International Ltd). Protein was eluted with a salt gradient from buffer *A* to buffer *B* (500 m*M* potassium phosphate buffer pH 7.0 containing 0.1 m*M* EDTA and 0.1 m*M* DTT). The preparation was about 95% pure at this stage as judged by visual inspection of an electrophoreogram. For crystallization experiments, the sample solution containing both α (CT and BCCP; MW 70 kDa) and β (BC; MW 50 kDa) subunits was dialyzed against 5 m*M* potassium phosphate buffer pH 7.0 containing 0.1 m*M* EDTA and 1 m*M* DTT and concentrated to 15 mg ml^{-1}.

2.3. Crystallization and X-ray data collection

A single crystal was grown by the hanging-drop vapour-diffusion method. To prepare each droplet, 15 mg ml^{-1} protein solution (2 µl; named PC-α+β) was mixed with 2 µl of a reservoir solution containing 20% polyethylene glycol 8000 (PEG 8000) in 100 m*M* Tris–HCl pH 8.0; the reservoir volume was 200 µl. After 5–10 d small crystals were visible which eventually reached dimensions of 0.2 × 0.2 mm with a plate-

Table 1
Data-collection statistics.

Values in parentheses are for the outermost shell (2.18–2.10 Å resolution).

Resolution range (Å)	50–2.2
No. measured reflections	245991
No. unique reflections	34674
Completeness (%)	99.9 (99.9)
Average $I/\sigma(I)$	57.2 (10.3)
R_{sym}† (%)	6.5 (25.4)
Cell lattice	Orthorhombic
Space group	$P2_12_12$
Unit-cell parameters (Å)	
a	92.4
b	122.2
c	59.0
Z	4

† $R_{sym} = (\sum |I - \langle I \rangle| / \sum |\langle I \rangle|) \times 100$.

Table 2
Structure-refinement statistics.

Values in parentheses are for the outermost shell (2.2–2.3 Å resolution).

Resolution range (Å)	20–2.2
R_{work}†	0.201 (0.221)
R_{free}‡	0.229 (0.259)
No. reflections used	34551
No. protein atoms	3558
No. solvent atoms	275
Average B factor (Å^2)	
All atoms	29.4
Protein atoms	28.9
Solvent atoms	34.0
R.m.s. deviations from ideality	
Bond lengths (Å)	0.006
Bond angles (°)	1.2
Torsion angles (°)	22.8

† R_{work} is calculated from 95% of the reflections used for refinement [$R_{work} = (\sum |F_{obs} - F_{calc}| / \sum |F_{obs}|)$]. ‡ R_{free} is calculated from 5% of the reflections excluded from refinement.

like shape. The crystal was stored in 100 m*M* Tris–HCl pH 8.0 with 30% PEG 8000 and 23% sucrose for a few minutes. The crystal was picked up and immediately cooled in a stream of nitrogen gas at 100 K using a Rigaku crystal-cooling device. Intensity data were collected at BL24XU-A (Hyogo beamline) of SPring-8 with a Rigaku R-AXIS V imaging-plate X-ray detector and were processed with *HKL*2000 (HKL Research Inc). The data set from the crystal was 99.8% complete to 2.2–20.0 Å resolution; other statistics are tabulated in Table 1.

2.4. Structure determination, model building and refinement

From the data collected, the unit-cell parameters were determined to be $a = 92.4$, $b = 122.1$, $c = 59.0$ Å. The molecular weight of PC-α+β is approximately 120 kDa (70 + 50 kDa). To estimate the number of protein molecules in the asymmetric unit, the volume occupied by the solvent in the crystal was calculated from the Matthews coefficient (Matthews, 1968). This was found to be 10.7% if a 120 kDa protein was contained in the asymmetric unit, implying that the crystal cannot accommodate a PC-α+β molecule (CT + BCCP and BC subunits). If the crystal contains one molecule of PC-α (CT + BCCP subunit) or PC-β (BC subunit), the estimated solvent volume would be 47.7 or 62.8%, respectively, and if the crystal contains two molecules of PC-β, it would be 25.6%. These results suggested that the crystal contains one molecule of PC-α or PC-β, but it could not be determined which.

The initial phase was determined by molecular replacement with the structure of an ACC mutant as a search model. The final solution reached by the *EPMR* program (Kissinger *et al.*, 1999) yielded one structure with highest correlation for the result of calculations against reflections in the resolution range 15.0–4.5 Å. The molecular structure thus obtained underwent several cycles of refinement with the *CNX* minimization protocol (Brünger *et al.*, 1998), giving an R factor of 0.33% against data in the resolution range 20.0–3.0 Å. These results revealed the crystal to be composed of one BC protomer (PC-β) of PC. Since the catalytic function of PC-β is analogous to that of ACC, it was expected that the two molecular structures were also similar.

This results shown that crystals containing only PC-β were grown from PC-α+β solution (a mixture of PC-α and PC-β). The exact reason for this unexpected observation is not known, but a subtle difference in the purification and crystallization conditions may be responsible. Although holo PC elutes at a position corresponding to an octamer with composition $\alpha_4\beta_4$ on gel filtration, its peak is broad or broader than those of BC alone (β_2) or CT alone (α_4) that elute later. This may suggest that holo PC is prone to dissociate into

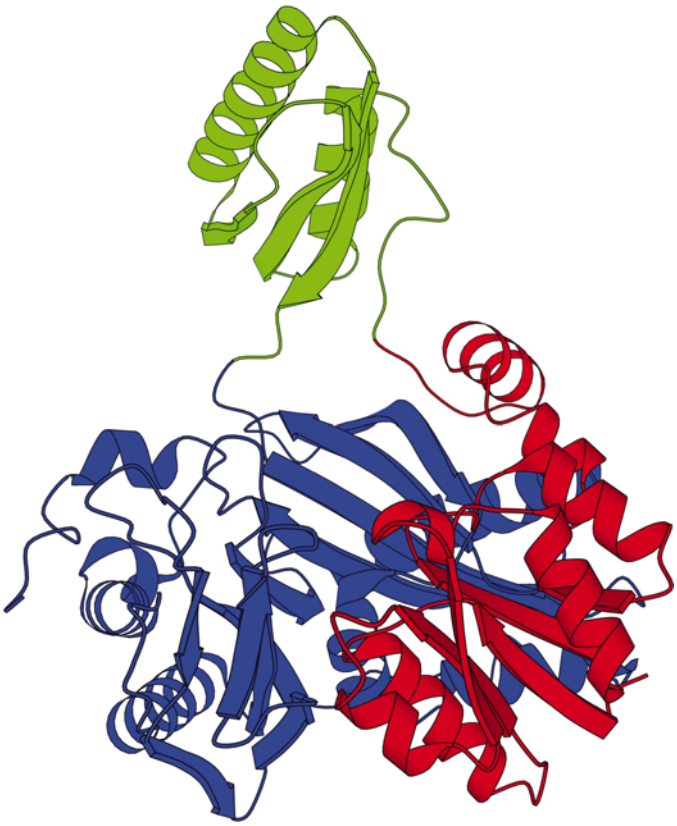

Figure 1
Overall schematic structure of PC-β illustrated by the program *MOLSCRIPT* (Kraulis, 1991). Domains *A*, *B* and *C* are shown in red, green and blue, respectively.

subunits even under mild conditions. In addition, the BC dimer may also be more prone to crystallize than the CT tetramer (in fact, we have yet to obtain a crystal of CT alone). Hence, holo PC may have undergone dissociation under 'harsher' crystallization conditions [pH 8.0 and 20%(*w*/*v*) PEG 8000].

The amino-acid residues of ACC used for the search were replaced with those of PC-β residues based on the computed results of homology alignment and the electron density of the initial phase. The rebuilt model structure underwent several cycles of refinement using the *CNX* slow-cooling protocol (Brünger *et al.*, 1998) against 20.0–3.0 Å resolution data. The calculated phases gave clear electron density for most of the residues except for the C-terminal regions and some parts of domain *B*. Composite omit-maps of domain *B* and the C-terminal region were calculated with the *CNX* protocol (Brünger *et al.*, 1998). The composite omit maps gave interpretable electron density. The model of domain *B* and the C-terminal region were manually revised with the program *XtalView* (McRee, 1993) and the entire model was refined at 20.0–2.2 Å resolution using *CNX* with options such as a target function MLF1 and a real-space bulk-solvent correction (Brünger *et al.*, 1998). The *R* factor and free *R* factor for the final model without solvent molecules were 0.29 and 0.32, respectively. The positions of solvent molecules were determined by the *CNX* water-pick protocol. *B*-factor refinement cycles for the model structures and the water molecules were carried out using the individual *B*-factor refinement protocol of *CNX*.

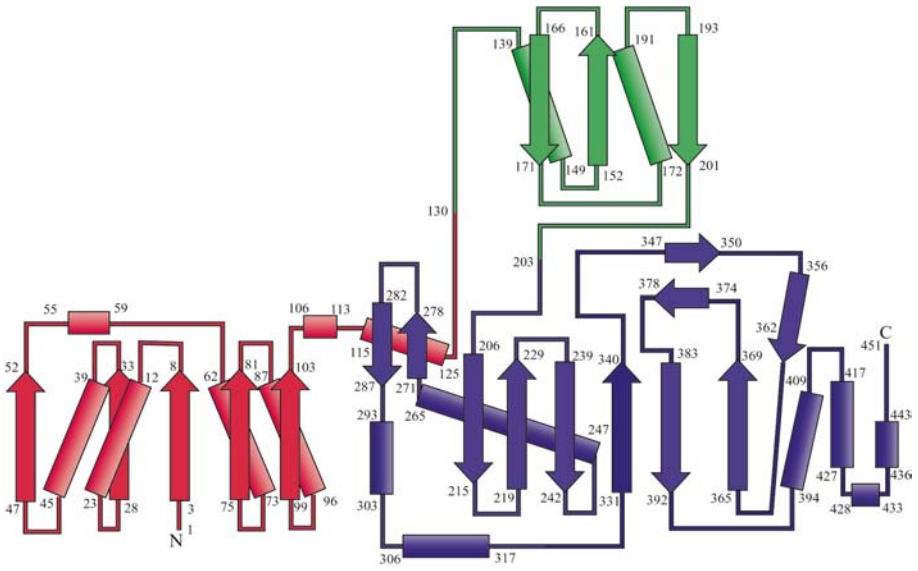

Figure 2
Topological diagram of PC-β. Domains *A*, *B* and *C* are shown in red, green and blue, respectively. The β-strands, α-helices and loop regions are shown by arrows, rectangles and lines, respectively. The first and last residues are shown as numbers next to each secondary-structure element.

3. Results and discussion

3.1. Quality of the structure

The asymmetric unit of a PC-β crystal contains one monomer of BC subunit, despite the crystal being grown from protein solution containing both CT + BCCP and BC subunits. The final atomic model consisted of 451 residues of PC-β (1–472) and 275 solvent molecules, giving an *R* factor and free *R* factor of 0.201 and 0.229, respectively. The statistics at the final refinement stage are shown in Table 2. Electron density is not clearly seen for residues Phe191–Arg193, Lys344–Lys345 and Pro349–Ser350 in the final $2F_{\rm obs} - F_{\rm calc}$ difference maps, probably owing to structural disorder. In a Ramachandran plot (Ramachandran & Sasisekharan, 1968), 88.6% of the residues fell in most favored regions as determined by the program *PROCHECK* (Laskowski *et al.*, 1993), but two residues (Phe83 and Asn269) fell in the generously allowed region. The latter observation is not an artefact, as the electron densities for both of these residues were very clear. Presumably, this anomalous conformation of the hydrophobic side chain of Phe83 was brought about to minimize its contact with the solvent, as this residue is at the protein surface. Although Asn269 is positioned away from the surface, it is surrounded by water molecules which seem to be associated with the anomalous conformation of Asn269. The root-mean-square deviations of the bond length, angle and torsion angle were in good agreement with the ideal values. Water molecules included in the final model gave an average *B* factor of 28.9 Å^2, which is comparable with those for main-chain atoms (27.8 Å^2) and side-chain atoms (29.7 Å^2).

3.2. Overall structure

The overall structure of PC-β is very similar to the BC of *E. coli* ACC. The overall folding of its polypeptide backbone is shown in Fig. 1. PC-β contains 16 α-helices and 19 β-strands; 40% of the residues are involved in α-helices and 30% of them in β-strands. A topological diagram showing the arrangement and naming of the secondary-structure element is presented in Fig. 2. PC-β consists of three domains, *A* (Met1–Val130), *B* (Pro131–Ile202) and *C* (Glu203-–Glu451), and its molecular architecture is similar to that of *E. coli* ACC (Waldrop *et al.*, 1994) or NAD$^+$-dependent dehydrogenases. The molecular dimensions of domains *A* and *C* are approximately 55 × 55 × 30 Å and that of domain *B* is approximately 22 × 28 × 25 Å. The N-terminal domain (domain *A*) consists of five β-strands of a parallel β-sheet and four α-helices which flank each side of the β-sheets. Domain *B* has two α-helices and three β-sheets and the glycine-loop region (residues 160–166) plays a crucial role in ATP binding (Thoden *et al.*, 2000). The C-terminal domain (domain *C*) consists of eight β-strands, an antiparallel β-sheet with half-barrel form, three other β-strands and seven α-helices. Those helices are situated at the back around

the barrel (Thr247–Ile265), inside (Gln293–Thr303), under (Asp306–Gly317) and near the C-terminus (Thr394–Tyr409, Thr417–Glu427, Lys428–Gly433, Thr436–His443).

PC-β has two *cis*-prolines, Pro153 and Pro242. Electron density for these residues was very clearly shown (Fig. 3) and they are conserved in ACC as well as in Pro155 and Pro244 (Waldrop *et al.*, 1994; Thoden *et al.*, 2000). Therefore, these residues seem to be important for forming the molecular structure of BC. Four methionine residues (Met112, Met122, Met273 and Met288) are located close to each other in PC-β with their S^{γ} atoms forming a cluster. In the BC of *E. coli* ACC (Kondo *et al.*, 1991), Met273 of PC-β is substituted by Phe275, so the cluster is not conserved. The cluster found in PC-β has a space large enough to accommodate a small molecule. No electron density was found in the hole, however, and it is not still clear what role if any the cluster is playing in PC-β. Contribution to the thermal stability of the protein may be one possibility.

3.3. Structure of domain *B*

Domain *B* extends from the main body (domains *A* and *C*) of PC-β and is constructed of a β-sheet with three strands and two α-helical units. As the role of this domain is to bind ATP, its structure is similar to those of proteins of the ATP-grasp family.

The structures of ACC alone (Waldrop *et al.*, 1994) and in complex with ATP have been determined (Thoden *et al.*, 2000). However, the structure of domain *B* of ACC alone was not completely revealed presumably owing to structural disorder (Waldrop *et al.*, 1994). Fig. 4 indicates that the domain arrangement of PC differs from that of ACC. PC-β can be superimposed on ACC, either alone or in complex with ATP, as shown in Figs. 4(*a*) and 4(*b*), respectively. Domain *B* of PC-β sits almost in the same position as that of *E. coli* ACC without substrate (open form), while domain *B* of ACC moves toward domain *A* when ATP is bound (closed form). Therefore, domain *B* of PC-β and that of ACC (closed form) are located quite differently, *i.e.* Ala190 of PC-β and Ala192 of ACC are 25.6 Å apart from one another. These two domains can be superimposed by a rotation of approximately 42° around residues Lys206 of PC-β and Arg208 of ACC, as the overall folding of the two domains is similar. These results indicate that the hinge-bending motion occurs between domain *B* and the rest of the molecule, but the conformational change of domain *B* itself is not remarkable upon ATP binding (Thoden *et al.*, 2000).

Domain *B* has a highly conserved glycine-loop region that acts as the ATP-binding site as in the BC domains of biotin-dependent enzymes (Kondo *et al.*, 1991). In PC-β, residues Ala160–Gly166 are identified as this region. Conformational changes of the glycine-loop occur that bury the bound ATP surface in ACC (Thoden *et al.*, 2000). Fig. 5 shows that domain *B* of PC-β superimposes on that of ACC and that the structures are virtually the same except for the glycine-loop region. It was expected that the backbone torsion angles (φ and ψ) of

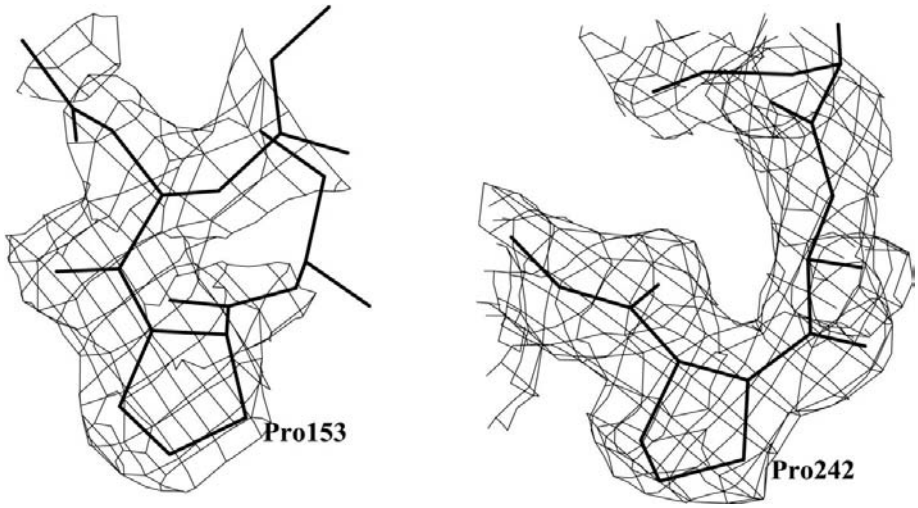

Figure 3
Electron densities of the *cis*-prolines of PC-β. Pro153 is shown on the left and Pro242 on the right. Electron densities for both are represented as $2F_{obs} - F_{calc}$ maps at 1.5σ contour with the final model.

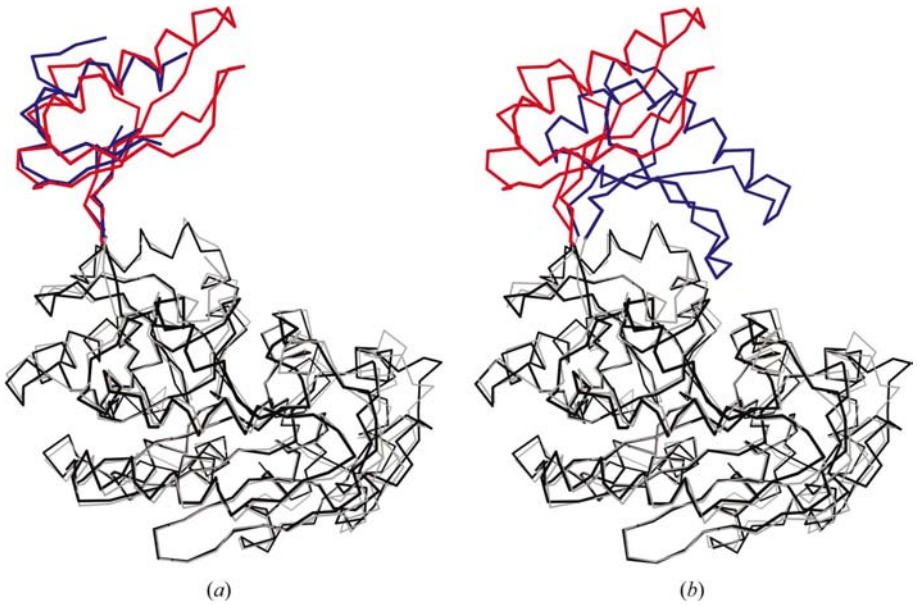

Figure 4
(*a*) C^{α} models of superpositioned PC-β and unligated ACC (open form). (*b*) C^{α} models of superpositioned PC-β and ligated ACC (ATP-bound; closed form). Structural superposition was made with only C^{α} atoms belonging to domains *A* and *C* in both PC-β and ACC (thick and thin black lines, respectively). Domain *B* of PC-β and ACC are shown in red and blue, respectively.

Table 3
List of backbone torsion angles in Gly-loop residues.

ACC (φ, ψ)	PC-β (φ, ψ)
Gly162 (−73.2, 0.4)	Ala160 (−156.1, 169.0)
Gly163 (76.8, −98.7)	Gly161 (80.1, 179.9)
Gly164 (83.2, −66.9)	Gly162 (−93.8, 10.3)
Gly165 (−178.1, 179.6)	Gly163 (−74.9, 171.8)
Gly166 (82.1, −15.3)	Gly164 (−60.8, 136.7)
Arg167 (−94.7, 33.1)	Arg165 (−98.1, −2.4)
Gly168 (94.5, 34.4)	Gly166 (−62.4, 145.5)

the glycine-loop region in PC-β would change to those found in ACC (as shown in Table 3) when ATP is bound to the enzyme if PC-β follows the same mechanism. From the structural comparisons described above, the glycine-loop is highly flexible as reflected by the fact that the open form of ACC does not clearly reveal the structure of the glycine-loop, while it is clearly observed in PC-β. One of the possible reasons for the difference is that Gly162 in ACC is substituted by Ala in PC-β (Ala160), which would restrict the conformational flexibility of the glycine-loop (Waldrop *et al.*, 1994).

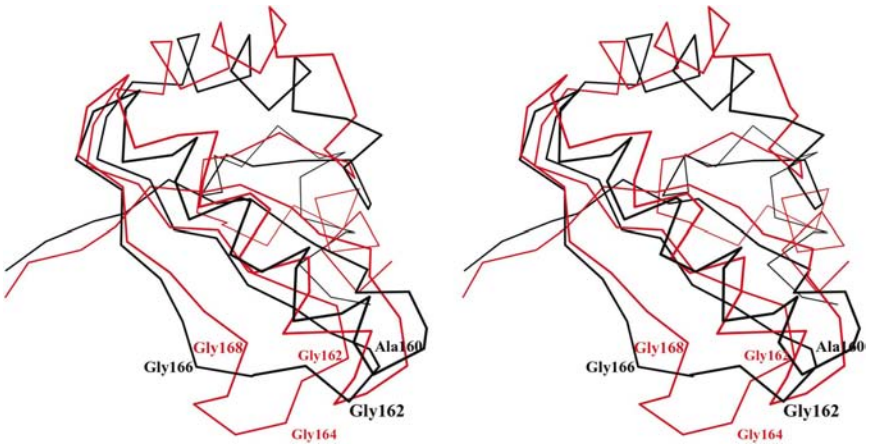

Figure 5
Stereoview of domain *B* of PC-β and ligated ACC (closed form). Domain *B* of ACC is obtained from the complex with ATP (Thoden *et al.*, 2000). The PC and ACC backbones are shown in black and red, respectively. Residues in the glycine-loops of PC-β (Gly160–Gly166) and ACC (Gly162–Gly168) are also labelled in black and red, respectively.

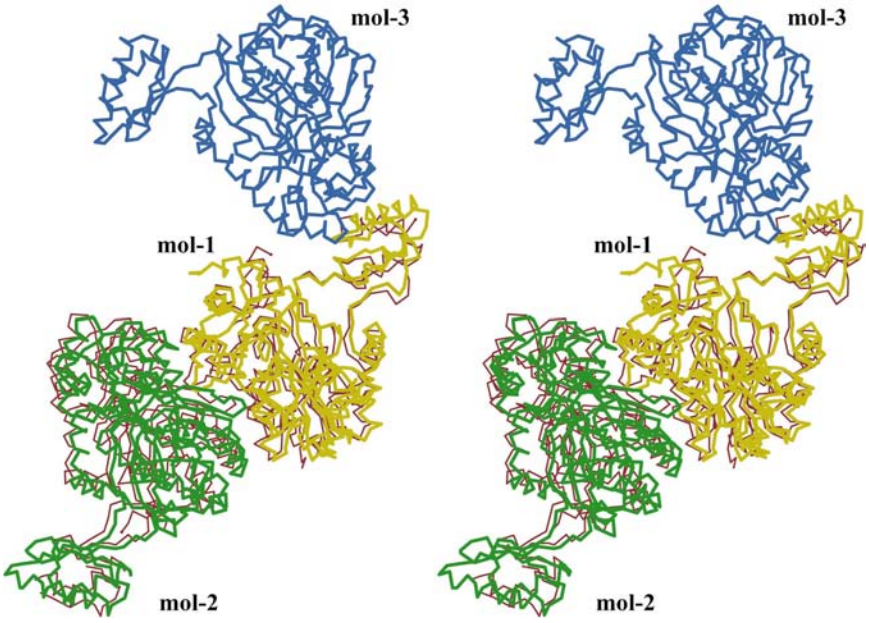

Figure 6
Stereoview of crystal packing for PC-β. The three monomers of PC-β found in the crystal structure are shown in yellow (mol-1), green (mol-2) and blue (mol-3). Each monomer belongs to a different asymmetric unit and mol-2 and mol-3 are generated by crystallographic symmetry operations: $(-x, -y, z)$ and $(\frac{1}{2} + x, \frac{1}{2} - y, -z)$, respectively. The dimeric structure of unligated ACC (Waldrop *et al.*, 1994) drawn as thin red lines is superimposed on the plausible dimer of PC-β (mol-1 and mol-2).

3.4. Quaternary structure and crystal packing

E. coli ACC has two molecules in the asymmetric unit and these molecules form a dimeric structure (Waldrop *et al.*, 1994; Thoden *et al.*, 2000). In the crystal structure of PC-β, on the other hand, there is one protein molecule in the asymmetric unit and two molecules are related by a crystallographic twofold symmetry (mol-1 at x, y, z and mol-2 at $-x$, $-y$, z), resulting in the formation of a dimer giving rise to an arrangement very similar to that found in ACC (Fig. 6). Another symmetry-related molecule (mol-3 at $\frac{1}{2} + x, \frac{1}{2} - y, -z$) is also proximal to mol-1 (Fig. 6). However, the contact area between mol-1 and mol-3 is much smaller than that between mol-1 and mol-2, so that the pair mol-1 and mol-3 does not look like a plausible dimer. These results indicate that the pair mol-1 and mol-2 is probably a real quaternary structure of PC-β found under physiological conditions.

3.5. ATP-binding site

Both PC-β and ACC belong to a superfamily of proteins characterized by an ATP-grasp fold (Galperin & Koonin, 1997). A multiple sequence alignment of PC-β and ACC revealed that residues in the catalytic and substrate-binding regions are highly conserved. The structure of ACC in complex with an ATP analogue has revealed the movement of domain *B* and the interactions between the active-site residues and ATP (Thoden *et al.*, 2000). Although the crystal structure of PC-β does not have any ATP analogues in its active site, the structure of ACC enables us to build a putative ATP complex of PC-β by superimposing conserved active-site residues (see caption of Fig. 7). A distinct structural difference is found in the loop region Phe201–Pro205 of PC-β (Fig. 7*a*) and

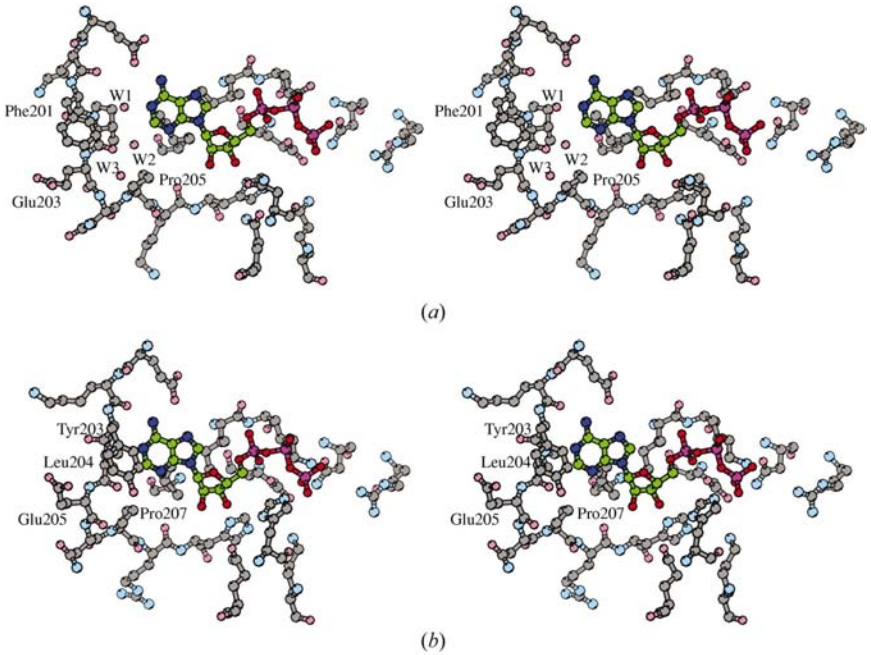

Figure 7
Stereoviews of the active-site structures (ball-and-stick models). The putative model of (*a*) PC-β and (*b*) ACC in complex with ATP (Thoden *et al.*, 2000). To construct the putative structure of PC-β, the crystal structures of PC-β and ACC were superimposed with C^{α} atoms of the residues Lys200, Phe201, Ile202, Glu203, Asn204, Pro205, Lys206, His207, Gln231, Ans234, Lys236, Glu274, Ile276, Ile286, Glu287, Asn289 and Arg291 in PC-β; the ATP molecule was then recruited from ACC and energy minimization was applied to the putative PC-β in complex with ATP using the program *DISCOVER* (Accerlys Inc.). C, O, N and P atoms of ATP are shown in green, red, blue and pink and C, N and O atoms of PC-β and ACC are shown in black, light blue and light red, respectively.

Tyr203–Pro207 of ACC (Fig. 7*b*). The peptide backbone between Glu203 and Gln204 in PC-β is flipped out compared with the corresponding part of ACC (Glu205 and Gln206) and the carbonyl O atoms of Glu203 in PC-β and Glu205 in ACC point in opposite directions (Figs. 7*a* and 7*b*). As a consequence, residues Phe201 and Ile202 move away from the adenine base-binding site in PC-β. In the putative complex of PC-β, three water molecules found in the crystal structure (W1, W2, W3 in Fig. 7*a*) could even occupy sites equivalent to Leu204 N, Leu204 O and Glu205 O in ACC (Fig. 7*b*), with r.m.s.d.s of 0.35, 0.70 and 1.61 Å, respectively. If PC-β interacts with ATP in a similar manner, it is likely that the water molecules are excluded and the loop moves toward the bound substrate by changing backbone torsion angles. It is not yet clear why single polypeptide-type PCs require acetyl-CoA for activation and we believe that crystal structure analysis of this class of PCs, such as that from *B. thermodenitrificans*, would help to clarify this question.

The authors are grateful to Ms Miwako Kawamoto for assistance in the construction of the recombinant plasmids. Thanks are also due to Professor Robert Huber of Universität Regensburg, Germany and his colleagues for the kind donation of *A. aeolicus* chromosomal DNA. The X-ray diffraction experiments were performed at BL24XU in Spring-8 with the approval of Hyogo Prefecture Government and the Japanese Synchrotron Radiation Research Institute (JASRI). This work was partially supported by 'National Project on Protein Structural and Functional Analyses' run by the Japanese Ministry of Education, Culture, Sports, Science and Technology.

References

Attwood, P. A. (1993). *Biochemistry*, **32**, 12736–12742.
Attwood, P. A. (1995). *Int. J. Biochem. Cell Biol.* **27**, 231–249.
Barden, R. E., Taylor, B. L., Isohashi, F., Frey, W. H., Zander, G., Lee, J. C. & Utter, M. F. (1975). *Proc. Natl Acad. Sci. USA*, **72**, 4308–4312.
Brünger, A. T., Adams, P. D., Clore, G. M., Delano, W. L., Gros, P., Grosse-Kunstleve, R. W., Jiang, J.-S., Kuszewski, J., Nilges, M., Pannu, N. S., Read, R. J., Rice, L. M., Simonson, T. & Warren, G. L. (1998). *Acta Cryst.* D**54**, 905–921.
Cazzulo, J. J. & Stoppani, A. O. (1968). *Arch. Biochem. Biophys.* **127**, 563–567.
Cohen, N. D., Duc, J. A., Beegen, H. & Utter, M. F. (1979). *J. Biol. Chem.* **254**, 9262–9269.
Deckert, G., Warren, P. V., Gaasterland, T., Young, W. G., Lenox, A. L., Graham, D. E., Overbeek, R., Snead, M. A., Keller, M., Aujay, M., Huber, R., Feldman, R. A., Short, J. M., Olsen, G. J. & Swanson, R. V. (1998). *Nature (London)*, **392**, 353–358.
Galperin, M. Y. & Koonin, E. V. (1997). *Protein Sci.* **6**, 2639–2643.
Jitrapakdee, S. & Wallace, J. C. (1999). *Biochem. J.* **340**, 1–16.
Kissinger, C. R., Gehlhaar, D. K. & Fogel, D. B. (1999). *Acta Cryst.* D**55**, 484–491.
Kondo, H., Kazuta, Y., Saito, A. & Fuji, K. (1997). *Gene*, **191**, 47–50.
Kondo, H., Shiratsuchi, K., Yoshimoto, T., Masuda, T., Kitazono, A., Tsuru, D., Anai, M., Sekiguchi, M. & Tanabe, T. (1991). *Proc. Natl Acad. Sci. USA*, **88**, 9730–9733.
Kraulis, P. J. (1991). *J. Appl. Cryst.* **24**, 946–950.
Laskowski, R. A., MacArthur, M. W., Moss, D. S. & Thornton, J. M. (1993). *J. Appl. Cryst.* **26**, 283–291.
McRee, D. E. (1993). *Practical Protein Crystallography*. New York: Academic Press.
Matthews, B. W. (1968). *J. Mol. Biol.* **33**, 491–497.
Mukhopadhyay, B., Stoddard, S. F. & Wolfe, R. S. (1998). *J. Biol. Chem.* **273**, 5155–5166.
Ramachandran, G. N. & Sasisekharan, V. (1968). *Adv. Protein Chem.* **23**, 283–437.
Scrutton, M. C. (1978). *FEBS Lett.* **89**, 1–9.
Thoden, J. B., Blanchard, C. Z., Holden, H. M. & Waldrop, G. L. (2000). *J. Biol. Chem.* **275**, 16183–16190.
Waldrop, G. L., Rayment, I. & Holden, H. M. (1994). *Biochemistry*, **30**, 10249–10256.
Wood, H. G. & Barden, R. E. (1977). *Annu. Rev. Biochem.* **46**, 385–413.
Zhang, H., Yang, Z., Shen, Y. & Tong, L. (2003). *Science*, **299**, 2064–2067.